

Lower Critical Solution Temperature Behavior of Poly(*N*-tetrahydrofurfuryl(meth)acrylamide) in Water and Alcohol–Water Mixtures

Yasushi Maeda* and Shinji Takaku

Department of Applied Chemistry and Biotechnology, University of Fukui, Fukui 910-8507, Japan

Received: August 1, 2010; Revised Manuscript Received: September 9, 2010

The temperature responsiveness of poly(*N*-tetrahydrofurfurylacrylamide) (PTHFA, phase transition temperature, $T_p = 38\text{ }^\circ\text{C}$) and poly(*N*-tetrahydrofurfurylmethacrylamide) (PTHFMA, $T_p = 43\text{ }^\circ\text{C}$) in water and alcohol–water mixtures was investigated by infrared and Raman spectroscopy. Their T_p increased monotonically with increasing concentration of added methanol but exhibited a re-entrant behavior in 1-propanol–water mixtures. Their amide I bands consist of three components because of doubly, singly, and zero hydrogen-bonding amide carbonyls in these mixtures, and the average number of hydrogen bonds per one C=O decreased with increasing concentration of the alcohols. A red shift of the amide II band also indicates decrease of H-bonding to the N–H group. The reduction then destabilizes the solution and lowers T_p . On the other hand, red shifts of the $\nu(\text{C–H})$ bands indicate replacement of hydrophobically hydrating water molecules by the alcohols, which may stabilize the solutions. The latter and the former effect may be more effective in the methanol–water and the 1-propanol–water mixtures, respectively. The behaviors of the copolymers of *N*-isopropylacrylamide and *N*-tetrahydrofurfurylacrylamide or *N*-tetrahydrofurfurylmethacrylamide in methanol–water mixtures gradually changed from a monotonous behavior to a reentrant one with an increasing content of *N*-isopropylacrylamide, suggesting that the interaction between each individual monomer unit and solvent molecules cooperatively determines their behaviors as a whole.

Introduction

Temperature-sensitive polymers are of great scientific importance and have recently received keen attention.¹ A variety of applications have also been reported ranging from controlled drug delivery systems to the separation of many kinds of compounds.² Aqueous solutions of these polymers undergo a thermally induced, reversible phase separation above phase separation temperatures (T_p), which depend on their structures. Poly(*N*-alkylacrylamides) such as poly(*N*-*n*-propylacrylamide) (PNPA, $T_p = 23\text{ }^\circ\text{C}$),³ poly(*N*-isopropylacrylamide) (PNiPAm, $31\text{ }^\circ\text{C}$),⁴ poly(*N*,*N*-diethylacrylamide) (PDEA, $31\text{ }^\circ\text{C}$),⁵ poly(*N*-cyclopropylacrylamide) (PcPA, $58\text{ }^\circ\text{C}$),³ and poly(*N*-ethylacrylamide, $74\text{ }^\circ\text{C}$)⁶ are typical examples. The balance between hydrophilicity and hydrophobicity is of primary importance to determine T_p . Their molecular weight and tacticity⁷ are also known to have effects on T_p .

The influence of additives on the phase behaviors has also been studied. It is known that PNiPAm exhibits cononsolvency in methanol–water mixtures. Though methanol is a good solvent for PNiPAm, the addition of methanol once reduces T_p of PNiPAm solutions to a minimum of $-7.5\text{ }^\circ\text{C}$ at 55 % (v/v) and then steeply raises T_p . The origin of the cononsolvency has been discussed for a long time. Among three kinds of interactions in the ternary system, the importance of the methanol–water interaction was once believed.⁸ Because the association of methanol to the amide groups of the polymer was proved recently by using IR spectroscopy,^{4,9} the importance of polymer–methanol interaction has been recognized. Tanaka et al. reported that the theoretical model based on competitive hydration bonding by water and methanol molecules to PNiPAm can explain the reentrant behavior.¹⁰ However, the mechanisms

of this behavior have not been fully understood on a molecular level. Though the cononsolvency of PNiPAm has been studied in detail, behaviors of other polymers^{5,11,12} are not known so well. To reveal the mechanism, it is important to compare the behaviors of several poly(*N*-alkyl(meth)acrylamides) and poly(*N*-alkoxy(meth)acrylamides) in some organic solvent–water mixtures as well as methanol–water mixtures.

Poly(*N*-alkoxy(meth)acrylamides) contain both amide and ether groups in each monomeric unit, and the additional ether groups make their phase behaviors different from those of poly(*N*-alkyl(meth)acrylamides) in some aspects.¹³ However, they have not been investigated so often. In the previous study, we investigated the behaviors of poly(*N*-(2-ethoxyethyl)acrylamide) (PEoEA, $T_p = 38\text{ }^\circ\text{C}$) and poly(*N*-(2-ethoxyethyl)methacrylamide) (PEoEMA, $T_p = 50\text{ }^\circ\text{C}$). Their T_p monotonously increased with increasing concentration of added methanol unlike the reentrant phase separation of PNiPAm. IR spectra showed that methanol interacts with both amide and alkyl groups. The interactions were qualitatively the same as those of PNiPAm, although PNiPAm has a higher tendency to accept double hydrogen bonds (H-bonds) at the C=O groups. In the present study, we investigate solvation and phase behaviors of other poly(*N*-alkoxy(meth)acrylamides), poly(*N*-tetrahydrofurfurylacrylamide) (PTHFA) and poly(*N*-tetrahydrofurfurylmethacrylamide) (PTHFMA), in water and alcohol–water mixtures by infrared and Raman spectroscopy.

Experimental Methods

Materials. *N*-Tetrahydrofurfurylacrylamide (THFA) and *N*-tetrahydrofurfurylmethacrylamide (THFMA) were synthesized via coupling of tetrahydrofurfurylamine (Wako) and acryloyl chloride or methacryloyl chloride (Wako) in the presence of triethylamine in benzene, respectively. Purification of these

* To whom correspondence should be addressed. Fax: +81-776-27-8747. E-mail: y_maeda@u-fukui.ac.jp.

monomers was carried out by vacuum distillation. *N*-Isopropylacrylamide (NiPAm) was kindly donated by Kohjin Co. Ltd. (Tokyo, Japan) and purified by recrystallization from benzene-*n*-hexane. PTHFA, PTHFMA, and copolymers of NiPAm and THFA or THFMA [P(THFA-NiPAm) or P(THFMA-NiPAm)] were synthesized via radical polymerization in methanol at 70 °C for 7 h using 2,2'-azobis(isobutyronitrile) as an initiator. After evaporation they were purified by dialysis against pure water (seamless cellulose tube, exclusion limit 12000) and were recovered by freeze-drying. Roughly estimated weight-average molecular weights (M_w) and polydispersity (M_w/M_n) of the polymers determined by gel permeation chromatography (column, Toso TSK gel GMH_{HR}-M; mobile phase, chloroform (0.6 mL·min⁻¹); standard, poly(ethyleneglycols)) were $M_w = 31\,000$ and $M_w/M_n = 2.5$ for PTHFA and $M_w = 20\,000$ and $M_w/M_n = 2.7$ for PTHFMA. The values for the copolymers were $M_w = 23\,000 - 41\,000$ and $M_w/M_n = 2.6 - 3.4$. They were dissolved in D₂O (Aldrich, 99.9%) and allowed to stand more than one day below T_p to equilibrate H-D exchange to prepare *N*-deuterated species.

Pure water, D₂O, methanol (MeOH), methanol-*d*₄ (MeOH-*d*₄), 1-propanol (1PrOH), and 2-propanol-*d*₈ (2PrOH-*d*₈) were used as solvents for the following measurements.

Measurements. IR spectra were measured at a resolution of 2 cm⁻¹ by using a Fourier transform infrared spectrometer (FTIR-8400, Shimadzu) equipped with a deuterated triglycine sulfate detector. Each polymer solution was placed between two CaF₂ windows directly (>50 wt %) or with a 10 μm thick spacer (≤50 wt %), and its temperature was controlled by using a circulating water bath. IR spectra of the solution were continuously collected at different temperatures at a heating rate of 0.5 °C/min. A difference spectrum ($\Delta A(\nu, T)$) was obtained by subtracting the IR absorption spectrum measured at the initial temperature from that measured at an elevated temperature (T).

Raman spectra were measured at a resolution of about 1 cm⁻¹ using a confocal micro-Raman spectrometer (NRS-1000, JASCO) equipped with an Ar laser (GLG2169, Showa Optronics) operated at 514.5 nm and an electronically cooled (-70 °C) charge-coupled detector (DU401FI, Andor). A pinhole aperture (50 μm) and a 100× objective lens give a spatial resolution of about 1 and 2 μm to the lateral and vertical direction, respectively. Sample solutions were placed between a slide glass and a cover glass and put on a metal plate thermostatted by circulating water bath. Point-by-point mapping was carried out using a motorized scanning stage controlled by computer.

Differential scanning calorimetry (DSC) measurements were performed using a microcalorimetry system (MicroCal Inc.) at a scanning rate of 0.75 °C/min.

DFT Calculations. Density functional theory (DFT) calculations were performed using Gaussian 98 at the B3LYP level with the 6-31G(d,p) basis set. The structure of the model for the monomer unit of PTHFMA is shown in Figure 1b. The methyl groups attached to both ends of the main chain, which are not included in the repeating unit of PTHFMA, were deuterated to remove unnecessary vibrational coupling with the remaining parts of the molecule. The amide proton was also deuterated if necessary. The serial numbers of atoms used to define vibration modes are shown in Figure 1a.

Results and Discussion

Phase Behavior of PTHFA and PTHFMA in Water. Aqueous solutions of PTHFA and PTHFMA became turbid above T_p of 38 and 43 °C (as onset temperatures), respectively (Figure 2a). T_p of PTHFMA, which has extra methyl groups,

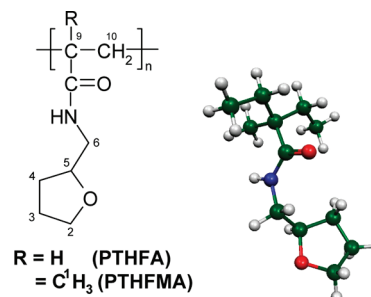


Figure 1. Structures of the polymers and the model compound of PTHFMA used for the DFT calculations.

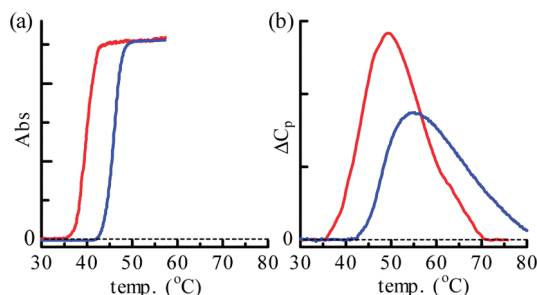


Figure 2. (a) Temperature dependence of turbidity (500 nm) of aqueous solutions of PTHFA (red) and PTHFMA (blue) ($W_p = 0.005$) at heating. (b) DSC thermograms of the solutions at heating.

was higher than that of PTHFA in a similar way that poly(*N*-isopropylmethacrylamide) (PiPMA, 46 °C) and poly(*N*-*n*-propylmethacrylamide) (32 °C) have higher T_p values than PNiPAm (31 °C) and PnPA (23 °C), respectively.¹⁴ The phase separation was accompanied by endothermic heat as shown in DSC thermograms of the solutions (Figure 2b) with an enthalpy of 8.0 and 7.4 J/g-polymer for PTHFA and PTHFMA, respectively. The transitions of PTHFA and PTHFMA (~25 °C) occurred in a much wider temperature region than those of PiPMA and poly(*N*-*n*-propylmethacrylamide) and are comparable to that of PdEA, indicating that the cooperativity of the dehydration of the polymers is low.¹⁵

The IR absorption spectra of the aqueous solutions of PTHFA and PTHFMA (weight fraction, $W_p = 0.1$) measured at temperatures below and above T_p are shown in Figure 3. The $\nu(\text{C-H})$ and amide I, II bands of their D₂O solutions and the $\delta(\text{C-H})$ and $\nu(\text{C-O})$ bands of their H₂O solutions are shown. The observed frequencies and the assignments based on the DFT calculations using the models are compiled in Table 1. Because the amide groups of these polymers were deuterated in D₂O, the amide II band (mainly due to N-H bending vibration) shifts from 1560 cm⁻¹ in H₂O to 1477 cm⁻¹ in D₂O and is referred to as the amide II' band. The difference spectra ($\Delta A(\nu)$) are also shown to enhance small changes in the frequency and absorbance of each band during phase separation. The $\nu(\text{C-H})$, amide II, $\delta(\text{C-H})$, and $\nu(\text{C-O})$ bands exhibit a red shift on the phase separation, while the amide I band exhibits a blue shift. These spectral changes will be discussed in more detail in the following section.

Progress of their hydration change can be visualized by plotting the values of $\Delta\Delta A(T) (= \Delta A(T, \nu_1) - \Delta A(T, \nu_2)$; ν_1 and ν_2 are the wavenumbers of positive and negative peaks in the difference spectrum) at some important vibration modes against temperature (Figure 4). The phase transition temperature (T_p) was given as onset temperatures of the $\Delta\Delta A(T)$ versus T plots. The value was close to its cloud-point temperature which was simultaneously measured via transmittance of visible light

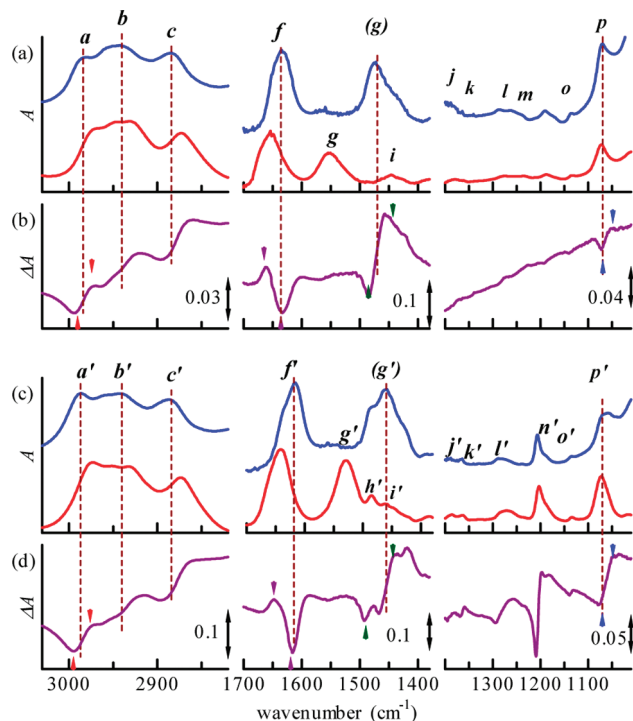


Figure 3. (a) IR absorption spectra ($A(\nu, 25^\circ\text{C})$) of PTHFA measured in solid state (red), D_2O ($W_p = 0.1$, $3030\text{--}2820\text{ cm}^{-1}$ and $1700\text{--}1380\text{ cm}^{-1}$) and H_2O ($W_p = 0.1$, $1400\text{--}1010\text{ cm}^{-1}$) (blue). (b) IR difference spectra ($\Delta A(\nu, 58^\circ\text{C}) = A(\nu, 58^\circ\text{C}) - A(\nu, 25^\circ\text{C})$) of PTHFA. (c) IR absorption spectra ($A(\nu, 25^\circ\text{C})$) of PTHFMA measured in solid state (red), D_2O ($W_p = 0.1$, $3040\text{--}2790\text{ cm}^{-1}$ and $1700\text{--}1380\text{ cm}^{-1}$) and H_2O ($W_p = 0.1$, $1400\text{--}1050\text{ cm}^{-1}$) (blue). (d) IR difference spectra ($\Delta A(\nu, 54^\circ\text{C}) = A(\nu, 54^\circ\text{C}) - A(\nu, 25^\circ\text{C})$) of PTHFMA. Vertical broken lines indicate the peak positions observed in D_2O . Triangles in the difference spectra indicate the position of the positive and negative peaks used to prepare Figure 4.

(ca. 510 nm). The onset temperatures of $\Delta\Delta A$ for the $\nu(\text{C-H})$, $\nu(\text{C-O})$, amide I, and amide II' modes agreed within experimental error, meaning that the dehydration of the corresponding groups of the polymer start at the same temperature as long as the present temperature resolution permits.

Optical microscopic observation shows that small particles appeared above T_p and gradually increased with increasing temperature. The image of the system ($W_p = 0.1$) observed at 50°C is shown in Figure 5a. A point-by-point Raman mapping was carried out using a motorized scanning stage, and the area ratio of the $\nu(\text{C-H})$ band of PTHFMA against $\nu(\text{O-H})$ band of water, $A_{\text{C-H}}/A_{\text{O-H}}$, is shown as a colored contour map (Figure 5b). The map indicates that the domain and the matrix are a polymer-rich phase and a solvent-rich phase, respectively.

We next measured Raman spectra at a fixed point in the domain phase to reveal temperature-induced change in polymer

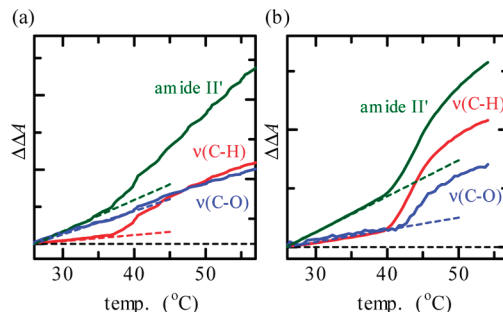


Figure 4. Values of $\Delta\Delta A(T) (= \Delta A(T, \nu_1) - \Delta A(T, \nu_2))$ for the $\nu(\text{C-H})$, amide II', and $\nu(\text{C-O})$ bands of (a) PTHFA and (b) PTHFMA in D_2O ($W_p = 0.1$) plotted against temperature. The positions of the negative and the positive peaks for the analyses are shown with triangles in Figure 3 parts b and d.

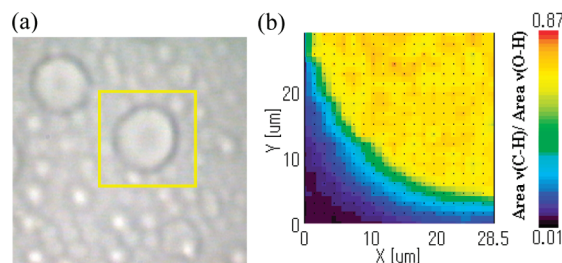


Figure 5. (a) Optical microscopic image of PTHFMA/ H_2O ($W_p = 0.1$) observed at 50°C . (b) A micro-Raman chemical map showing the value of $A_{\text{C-H}}/A_{\text{O-H}}$ of the system.

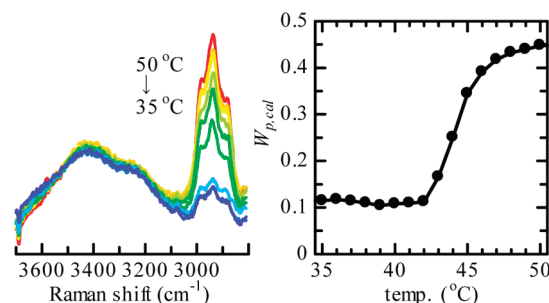


Figure 6. (a) Change of Raman spectra of PTHFMA/ H_2O ($W_p = 0.1$) observed in the domain phase at cooling ($50\text{--}35^\circ\text{C}$). (b) The value of $W_{p,\text{cal}}$ of PTHFMA in the domain phase at cooling is plotted against temperature.

concentration. The measurement was performed at a cooling process because of experimental easiness. An estimated weight fraction of PTHFMA ($W_{p,\text{cal}}$) is plotted against temperature in Figure 6. The value of $W_{p,\text{cal}}$ reached 0.47 at the highest temperatures of the measurements. The polymer concentration decreases with decreasing temperature at $50\text{--}42^\circ\text{C}$. Below T_p the value of $W_{p,\text{cal}}$ becomes independent of the position in the mixtures and also temperature.

TABLE 1: Observed IR Frequencies (cm^{-1}) and Assignments of PTHFA and PTHFMA in Water and Bulk State

PTHFA			PTHFMA		
neat	aqueous solution	assignment	neat	aqueous solution	
2970	2980	$\nu_{\text{as}}(\text{C}^6\text{H})$, $\nu_{\text{as}}(\text{C}^4\text{H})$, $\nu_{\text{as}}(\text{C}^1\text{H})^b$, $\nu_{\text{as}}(\text{C}^3\text{H})$	2973	2987	
2945	2951	$\nu_{\text{as}}(\text{C}^{10}\text{H})$, $\nu_{\text{as}}(\text{C}^2\text{H})$	2953	2957	
2931	2943	$\nu_{\text{s}}(\text{C}^4\text{H})$, $\nu_{\text{s}}(\text{C}^6\text{H})$, $\nu_{\text{s}}(\text{C}^3\text{H})$, $\nu_{\text{s}}(\text{C}^1\text{H})^b$, $\nu_{\text{s}}(\text{C}^{10}\text{H})$	2933	2942	
2873	2885	$\nu_{\text{s}}(\text{C}^9\text{H})^a$, $\nu_{\text{s}}(\text{C}^2\text{H})$, $\nu_{\text{s}}(\text{C}^5\text{H})$	2874	2887	
1654	1636	$\nu_{\text{s}}(\text{C}=\text{O})$	1641	1617	
1555	1473	$\delta(\text{N-D})$	1529	1459	
1072	1070	$\nu_{\text{as}}(\text{C-O-C})$	1071	1068	

^a Only for PTHFMA; ^b Only for PTHFA.

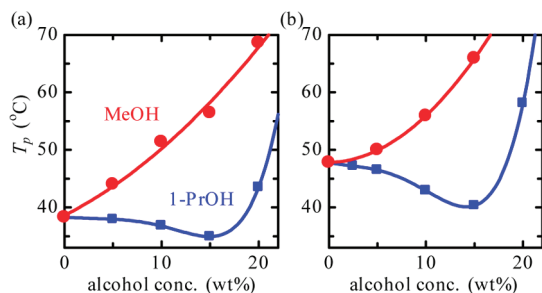


Figure 7. T_g of (a) PTHFA and (b) PTHFMA are plotted against alcohol concentration (●: methanol; ■: 1-propanol).

Effects of Alcohols on Phase Behavior. The effects of alcohols on T_g of PTHFA and PTHFMA were investigated (Figure 7). T_g of these polymers increased with MeOH concentration with a similar way to those of PdEA⁴ and poly(*N*-vinylcaprolactam).¹³ The behavior is, however, different from that of PNIPAm and other poly(*N*-monoalkylacrylamides), whose T_g in methanol–water mixtures passes through a minimum (-7.5 °C at 55 % v/v for PNIPAm).^{16,17} We had expected that the presence of the amide N–H group as H-bond donor is important for the influence of methanol on the phase behavior. The presence of the ether group and/or the whole difference in their side groups converts the reentrant behavior to the monotonous one. On the other hand, these polymers exhibited a reentrant phase behavior in 1-propanol–water mixtures.

We next measured IR spectra of PTHFA and PTHFMA in the mixed solvents to elucidate the polymer–solvent interactions. Figure 8 shows the $\nu(\text{C–H})$ and the amide bands of PTHFMA measured in MeOH- d_4 /D₂O of different compositions at 25 °C (homogeneous solutions).

As for the effects of methanol on the $\nu(\text{C–H})$ frequencies, they linearly decreased with increasing methanol concentration (Figure 9). The result suggests that the alkyl groups of PTHFMA are surrounded by methanol. Moreover, 2PrOH- d_8 has stronger effects on the shifts of the $\nu(\text{C–H})$ bands than methanol, indicating that it interacts with the alkyl groups of PTHFMA more effectively.

The addition of methanol alters the profile of the amide I bands of PTHFMA. A peak separation method was applied to the amide I bands to confirm H-bonding to the amide C=O groups (Figure 10). The amide I band of PTHFMA consists of three components centered at 1662, 1632, and 1616 cm^{-1} . We hereafter call the higher-, medium-, and lower-wavenumber components as comp-0, -1, and -2, respectively. Each of the

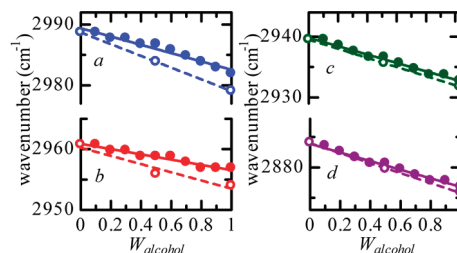


Figure 9. Wavenumbers of the peak a–d of PTHFMA measured in MeOH- d_4 /D₂O (●) and 2PrOH- d_8 /D₂O (○) at 25 °C plotted against W_{alcohol} .

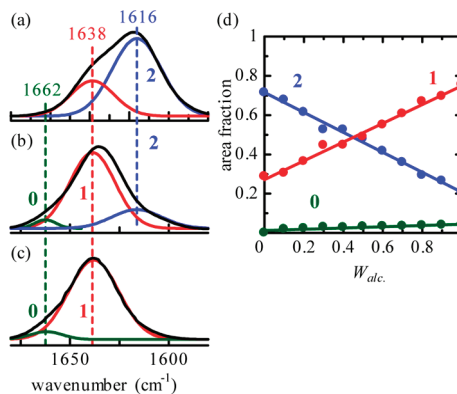


Figure 10. Amide I bands of PTHFMA ($W_p = 0.1$) measured in (a) D₂O, (b) MeOH- d_4 , and (c) 2PrOH- d_8 were dissolved into three Gaussian components. (d) The area fractions of the components in MeOH- d_4 /D₂O mixtures are plotted against methanol concentration.

amide I components of PTHFMA appears at a slightly lower frequency than the counterpart of PTHFA. It is known that the amide I components of PiPMA¹¹ also exist at lower frequencies than those of PNIPAm.^{3b} The methyl groups of PTHFMA and PiPMA affect the electron distribution on the amide groups and their vibration frequencies. The observation is supported by our DFT calculations.

Because H-bonding to an amide C=O group reduces electron density on the C=O bond, the frequency of the amide I mode which is mainly due to the C=O stretching vibration becomes low. When the number of H-bonds to the carbonyl becomes higher or the H-bonds become stronger, the frequency of the amide I modes becomes lower. Because the amide C=O group can accept up to two H-bonds, the comp-2 and the comp-1 can be assigned to the doubly and singly H-bonding C=O groups, respectively. Because the comp-0 is the main component of a dry polymer film, it can be assigned to the non-H-bonding C=O

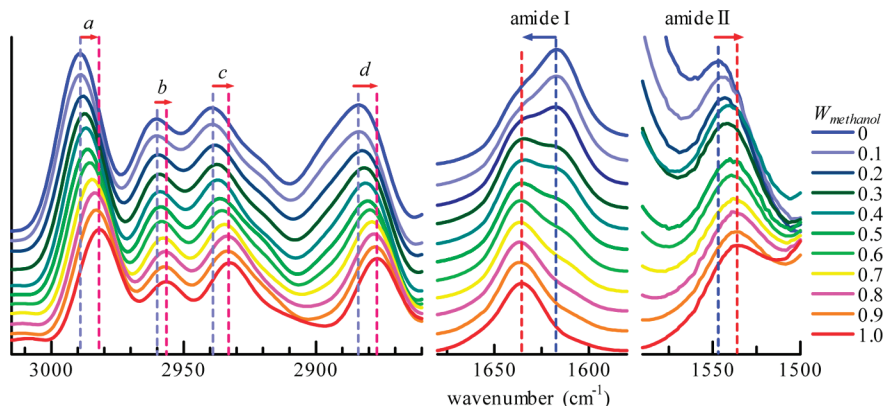


Figure 8. IR spectra of PTHFMA at (a) the $\nu(\text{C–H})$, (b) the amide I, and (c) the amide II modes measured in MeOH- d_4 /D₂O (a, b) and MeOH/H₂O of different compositions (weight fraction of the alcohol; $W_{\text{alcohol}} = 0$ –1) at 25 °C.

groups. Figure 10c shows that the area of the comp-1 increases and that of the comp-2 decreases with an increasing concentration of methanol, indicating that the average number of H-bonds to the amide groups of the polymer is reduced as methanol replaces water. Recent molecular dynamics simulations on the solvation of NiPAm in methanol–water mixtures also showed that the average number of H-bonds to the amide groups decreases with increasing concentration of methanol.¹⁸ A small and negligibly small contribution of the comp-2 in methanol and 2-propanol means that it is difficult for two alcohol molecules to bind to one C=O group of PTHFA probably because of a steric effect of their alkyl groups. Moreover, a comparison of the amide bands of the two polymers reveals that the area fraction of the comp-2 of PTHFA is higher than that of PTHFMA at any compositions. The fact means that the C=O groups of PTHFA have a stronger tendency to accept two H-bonds than those of PTHFMA.

The H-bonding to the amide N–H of the polymers can be estimated from the amide II band (Figure 9). The band arises from combination of N–H bending and C–N stretching vibrations. The N–H (or N–D) groups will act as H-bond donor (N–H···OH₂). The H-bond holds the amide proton and increases the force constant of the vibration, which causes a blue shift of the amide II band. The band exhibited a red shift with increasing concentration of methanol. The shift indicates a reduction of the number of H-bonds to the N–H group.

Because an alcohol molecule has both a polar hydroxyl group and an apolar alkyl group, it can interact with both polar and apolar sites of polymers. When the amide groups of the polymer interact with the alcohol molecules through H-bond (C=O···H–O–H, N–H···OH₂), the average number of H-bonds to the amide groups is reduced, and the total surface area of hydrophobic site increases. The polymer is destabilized in water, and finally T_p is reduced. The effect is more significant with 2PrOH than with methanol. When apolar sites of the polymer interact with the alcohol molecules through hydrophobic interaction, the system is stabilized, and T_p is raised. The balance of the two opposite effects may finally determine the T_p of the system.

Phase Behaviors of Copolymers. We prepared copolymers of NiPAm and THFA or THFMA of different compositions to investigate what occurs in their T_p when two different monomer units coexist in a single polymer chain. The values of T_p for the homopolymers and the copolymers in the alcohol–water mixtures are plotted against MeOH and 1PrOH concentration (vol %) (Figure 11). Dependence of T_p on alcohol concentration gradually changes with monomer contents. The copolymers with NiPAm contents of 0.75 clearly exhibit reentrant phase separation in methanol–water mixtures. As for 1PrOH–water mixtures, the minima become deep with increasing contents of NiPAm. The result suggests that cumulative effects of the interaction between each individual monomer unit and solvent molecules determine the behavior of the polymer as a whole.

Conclusions

Phase separation of PTHFA and PTHFMA in aqueous solutions has been investigated by infrared and Raman spectroscopy. Their phase behaviors were different from that of PNiPAm and other poly(*N*-alkyl(meth)acrylamides) in some aspects. They had a wide transition temperature region (~30 °C) instead of a sharp one (PNiPAm, ~1 °C) and did not exhibit cononsolvency in methanol–water mixtures. However, they showed cononsolvency in propanol–water mixtures. IR spectra indicated that these polymers interact with the alcohols both at

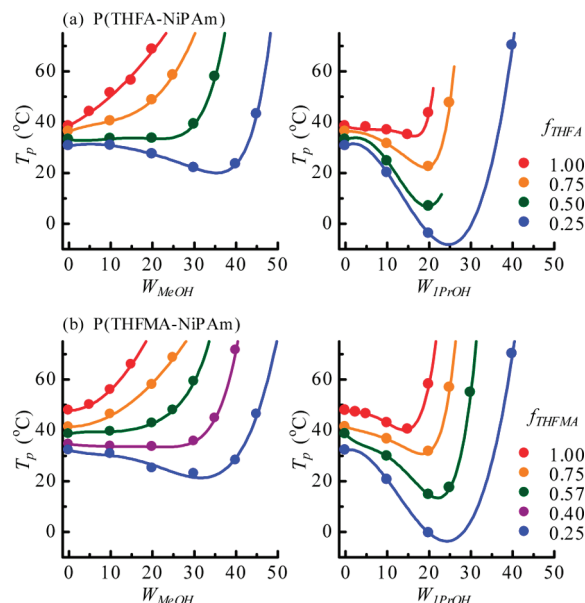


Figure 11. Values of T_p of (a) P(THFA-NiPAm) and (b) P(THFMA-NiPAm) of different composition in MeOH/H₂O (right) and 1PrOH/H₂O (left) are plotted against W_{alcohol} .

amide and alkyl groups. H-bonding of the alcohols to the amide groups of the polymer destabilizes the system and lowers T_p and solvation of the alcohols to the alkyl groups of the polymer stabilizes the system and raises T_p . Though H-bonding to the ether oxygen may have additional effects in the case of poly(*N*-alkoxy(meth)acrylamides), small spectral changes in the ether bands make it difficult to analyze hydration change at the site. The balance of among these effects may finally determine the T_p of the system. Because the copolymers of NiPAm and THFA or THFMA behave somewhere between PNiPAm and PTHFA or PTHFMA in the mixed solvents, we can say that cumulative effects related to the interaction between each individual monomer unit and solvent molecules finally determine the behaviors of the copolymers as a whole.

Acknowledgment. This work was supported by a Grant-in-Aid for Scientific Research (20550109) from Japan Society for the Promotion of Science.

References and Notes

- (1) (a) Schild, H. G. *Prog. Polym. Sci.* **1992**, *17*, 163. (b) Spěváček, J. *Curr. Opin. Colloid Interface Sci.* **2009**, *14*, 184.
- (2) (a) You, Y.-Z.; Kalebaila, K. K.; Brock, S. L.; Oupický, D. *Chem. Mater.* **2008**, *20*, 3354. (b) Reddy, T. T.; Kano, A.; Maruyama, A.; Hadano, M.; Takahara, A. *Biomacromolecules* **2008**, *9*, 1313. (c) Castellanos, A.; DuPont, S. J.; Heim, A. J., II; Matthews, G.; Stroot, P. G.; Moreno, W.; Toomey, R. G. *Langmuir* **2007**, *23*, 6391.
- (3) Maeda, Y.; Nakamura, T.; Ikeda, I. *Macromolecules* **2001**, *34*, 1391.
- (4) (a) Heskins, M.; Guillet, J. E. *J. Macromol. Sci., Chem.* **1968**, *A2*, 1441. (b) Fujishige, S.; Kubota, K.; Ando, I. *J. Phys. Chem.* **1989**, *93*, 3311.
- (5) Maeda, Y.; Higuchi, T.; Ikeda, I. *Langmuir* **2000**, *16*, 7503.
- (6) Maeda, Y.; Nakamura, T.; Ikeda, I. *Macromolecules* **2002**, *35*, 10172.
- (7) Taylor, L. D.; Cerankowski, L. D. *J. Polym. Sci., Part A: Polym. Chem.* **1975**, *13*, 2521.
- (8) Mori, T.; Hirano, T.; Maruyama, A.; Katayama, Y.; Niidome, T.; Bando, Y.; Ute, K.; Takaku, S.; Maeda, Y. *Langmuir* **2009**, *25*, 48.
- (9) (a) Amiya, T.; Hirokawa, Y.; Hirose, Y.; Li, Y.; Tanaka, T. *J. Chem. Phys.* **1987**, *86*, 2375. (b) Katayama, S.; Hirokawa, Y.; Tanaka, T. *Macromolecules* **1984**, *17*, 2641. (c) Hirotsu, S. *J. Phys. Soc. Jpn.* **1987**, *56*, 233. (d) Hirotsu, S. *J. Chem. Phys.* **1988**, *88*, 427.
- (10) Katsumoto, Y.; Tanaka, T.; Ihara, K.; Koyama, M.; Ozaki, Y. *J. Phys. Chem. B* **2007**, *111*, 12730.

- (10) Tanaka, F.; Koga, T.; Winnik, F. M. *Phys. Rev. Lett.* **2008**, *101*, 028302.
- (11) Maeda, Y.; Nakamura, T.; Ikeda, I. *Macromolecules* **2002**, *35*, 217.
- (12) Kouřilová, H.; Hanyková, L.; Spěvák, J. *Eur. Polym. J.* **2009**, *45*, 2935.
- (13) (a) Wada, N.; Yagi, Y.; Inomata, H.; Saito, S. *Macromolecules* **1992**, *25*, 7220. (b) Ito, S. *Kobunshi Ronbunshu* **1990**, *47*, 487.
- (14) Maeda, Y.; Nakamura, T.; Ikeda, I. *Macromolecules* **2001**, *34*, 8246.
- (15) Okada, Y.; Tanaka, F. *Macromolecules* **2005**, *38*, 4465.
- (16) Winnik, F. M.; Ringsdorf, H.; Venzmer, J. *Macromolecules* **1990**, *23*, 2415.
- (17) Schild, H. G.; Muthkumar, M.; Tirrell, D. A. *Macromolecules* **1991**, *24*, 948.
- (18) Pang, J.; Yang, H.; Ma, J.; Cheng, R. *J. Phys. Chem. B* **2010**, *114*, 8652.

JP1072268